

Reviewed Preprint

v1 • July 3, 2026

Not revised

✉ For correspondence:

christopher.larock@emory.edu

Competing interests: No

competing interests declared

Funding: See [page 20](#)

Reviewing editor: Edward A Miao, Duke University, United States

© 2026, Guerra et al. This article is distributed under the terms of the [Creative Commons Attribution License](#), which permits unrestricted use and redistribution provided that the original author and source are credited.

A protease-sensing circuit links neutrophil inflammation to virulence regulation in *Streptococcus pyogenes*

Stephanie Guerra^{1,2}, Ananya Dash^{1,3}, Doris L LaRock¹, Christopher N LaRock^{1,4} ✉¹Department of Microbiology and Immunology, Emory University School of Medicine, Atlanta, United States •²Microbiology and Molecular Genetics Program, Laney Graduate School, Emory University, Atlanta, United States •³Immunology and Molecular Pathogenesis Program, Laney Graduate School, Emory University, Atlanta, United States •⁴Division of Infectious Diseases, Department of Medicine, Emory University School of Medicine, Atlanta, United States

eLife Assessment

The authors describe a **valuable** finding that the *Streptococcus pyogenes* secreted protease SpeB is expressed in response to protease activity that degrades the Vfr repressor. Proteases can be released from host neutrophils (possibly by NETosis), as well as a positive feedback mechanism by SpeB itself. The authors utilize a dual fluorescent reporter system to simultaneously read *SpeB* and capsule gene expression, providing **solid** evidence that demonstrates that proteases can regulate Vfr; however, the data indicating that this is physiologically relevant and that extracellular traps themselves have a functional role are **incomplete**. This work will be of interest to microbiologists studying the regulation of virulence factors at the host-pathogen interface.

<https://doi.org/10.7554/eLife.112023.1.sa3>

Abstract

Streptococcus pyogenes (Group A *Streptococcus*) causes infections with a disproportionately hyperinflammatory response from the host, such as scarlet fever, necrotizing fasciitis, and toxic shock syndrome. Inflammation is specifically driven by *S. pyogenes* virulence factors, including the protease SpeB, but how inflammation impacts SpeB expression in return during disease is unknown. In this study, we identify a novel interaction between NETosis, a form of inflammatory cell death for neutrophils, and the induction of *speB*. Specifically, while the cathelicidin peptide LL-37 can repress *speB* through the two-component regulatory system CovRS, neutrophil proteases released during NETosis relieve repression of *speB* by degrading another repressor of *speB*, the bacterial protein Vfr. Furthermore, at high cell densities, SpeB autoregulates its expression through similar degradation of Vfr. Abrogating the formation of NETs or depleting neutrophils resulted in *speB* repression *in vivo*, showing the mutual host and pathogen counterattacks collectively lead to the pathological exacerbations characteristic of disease.

Introduction

Streptococcus pyogenes (*Spy*; Group A *Streptococcus*) is a human-exclusive bacterial pathogen responsible for billions of infections and more than 500,000 deaths annually, making it one of the top ten infectious causes of human mortality worldwide¹. Most infections are relatively mild, such as impetigo and pharyngitis, but serious, and often fatal diseases like bacteremia, puerperal sepsis, Streptococcal toxic shock syndrome (STSS), and necrotizing fasciitis arise when *Spy* becomes invasive. Virulence factors play a major role in disease progressing by facilitating tissue invasion, evading immune cell killing, and creating intracellular reservoirs⁶.

SpeB is a major virulence factor conserved amongst *Spy*, and is essential for colonization and proliferation within tissue in a variety of infection models⁷. Nonetheless, mutants arise during severe infections that, enigmatically, no longer express *speB*^{8,9}. These mutations are most commonly in the two-component system CovRS (CsrRS), which modulates expression of nearly 15% of *Spy* genes, including most virulence factors^{10–12}. CovRS senses the host cathelicidin peptide LL-37, produced by epithelial and immune cells as part of innate immune defense and wound repair^{5,13–15}. Loss-of-function *covRS* mutations dysregulate their virulence factors in a manner similar to constitutive LL-37 induction, decreasing production of SpeB, while increasing production of capsule (through the *hasABC* operon) and toxins like SLO, NADase, Mac/IdeS, and *...*. The major inducer of *speB* is RopB in response to the quorum-sensing peptide SIP^{16,17}. *In vitro*, the virulence factor-related (Vfr) protein also appears to antagonize induction, on the basis that *vfr* mutants express greater *speB*^{18,19}. How the combination of these possible host and microbial signals are integrated to regulate SpeB during infection is unknown.

This work shows that *Spy* establishes a phenotypically diverse population during infection through the heterogeneous expression of *speB*. Using genetics, RopB, Vfr, and the CovRS system are all found to be essential for generating discrete SpeB-producing and non-producing subpopulations. We show that Vfr is a labile sensor of protease activity that is degraded by SpeB, allowing it to autoregulate its own expression by relieving Vfr repression. Furthermore, neutrophil serine proteases also relieve Vfr repression, allowing the bacteria to sense both influx of neutrophils and their activities, with maximal *speB* induction occurring in response to neutrophil extracellular traps (NETs). Despite neutrophils being the major producers of LL-37, which can lead to *speB* repression through CovRS, protease sensing by Vfr ensures SpeB, which is important for resisting neutrophil-produced antimicrobials including LL-37²⁰, is still expressed in its presence. Together, our results show how *Spy* navigates the challenge of expressing the right virulence factor at the right time by use of a circuit that integrates host and microbial cues.

Results

S. pyogenes establishes subpopulation heterogeneity in their expression of *speB*

To examine *speB* expression within *Spy*, we generated a transcriptional fusion of *gfp* with 1000 bp upstream of the *speB* to include P1 and P2 regions of the *speB* promoter¹⁶. The best-characterized regulator of *speB* is CovRS; *speB* is derepressed when CovR is phosphorylated (CovR~P), in contrast to the capsule biosynthesis operon *hasABC*, which is induced when CovR is unphosphorylated¹². CovR phosphorylation depends on the histidine kinase, CovS, which is sensitive to environmental signals. To examine the contribution of *speB* inducers separate from this repressor, we created a tandem reporter that also has the *hasABC* promoter fused to *rfp*²¹ (Fig. 1A [↗](#)). To test the accuracy and precision of the reporter construct, *Spy* was grown in concentrations of LL-37 (300 nM) or MgCl₂ (15 mM) that did not impact bacterial growth (Fig. S1A [↗](#)), but which divergently regulate CovR phosphorylation of CovS¹². As expected for a quorum-sensing regulated protease¹⁷, GFP (*speB*) is induced as *Spy* approaches late log phase. The addition of LL-37 induced RFP (*hasABC*) and repressed both the expression of GFP (*speB*) (Fig. 1C [↗](#)) as well as production of the mature, active protease (Fig. S1B [↗](#)). Contrarily, GFP (*speB*) induction was maintained in the presence of MgCl₂, but RFP (*hasABC*) repressed. Examination by fluorescence microscopy recapitulated these observations, but suggested heterogeneity in these responses within the bacterial population (Fig. 1B [↗](#)).

To quantify this at the single-cell level, we next used flow cytometry. Size, BactoView™ Dead 760/780, and an antibody against the *Spy*-specific antigen Group A Carbohydrate (anti-GAC), were used to gate on single, live cells (Fig. S1C [↗](#)). As expected, *Spy* grown with LL-37 had a population shift positive for RFP and negative for GFP (Fig. 1D [↗](#)). Conversely, growth with MgCl₂ resulted in a lower and rightward shift in the population. However, there was significant heterogeneity even in these induced conditions, with large populations of intermediate expression.

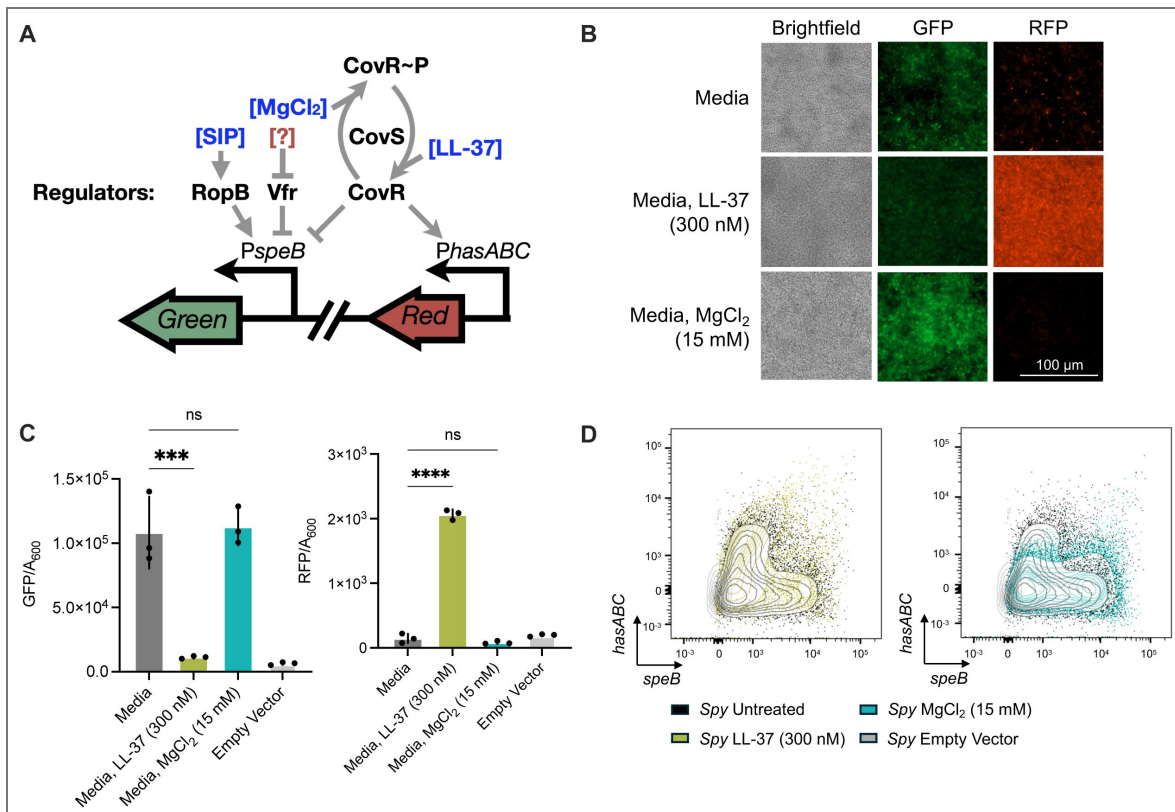


Fig. 1. *S. pyogenes* establishes subpopulation heterogeneity in their expression of *speB*.

(A) *speB* regulatory circuit schematic. RopB induces *speB* expression in the presence of SIP peptide and Vfr inhibits *speB* expression by blocking RopB-SIP complex. CovS kinase-mediated CovR phosphorylation (CovR~P) derepresses *speB*, while CovS phosphatase-mediated CovR dephosphorylation represses *speB*. MgCl₂ and LL-37 mediate CovS kinase and phosphatase, respectively. Induction of *speB* expression was evaluated with GFP fluorescence and *hasABC* expression was evaluated with RFP fluorescence. (B, C, D) Wild-type *Spy* was treated with LL-37 (300 nM) or MgCl₂ (15 mM). (B) Live-cell fluorescent microscopy with brightfield, GFP, and RFP channels on *Spy* culture grown at stationary phase. Scale bars, 100 μm. (C) Measurement of fluorescence over cell density after 10 h of growth. (D) Flow cytometry demonstrating *speB* expression (GFP; horizontal axis) and *hasABC* expression (RFP; vertical axis) of *Spy* growing at stationary phase. Statistical significance was determined using a one-way ANOVA with Dunnett's multiple comparisons test. ****P<0.0001, ***P<0.001, ns: not significant.

Genetic knockouts of known and probable SpeB regulators (Fig. 1A) were created to further validate the fluorescent reporters while defining determinants of heterogeneity. None impacted bacterial growth (Fig. S2A). A $\Delta covS$ mutant constitutively expressed high *hasABC*, (RFP), while repressing *speB*, as expected. A $\Delta ropB$ mutant did not express *speB*, in agreement with its reported importance for *speB* induction¹⁷. Interestingly, a $\Delta speB$ mutant also showed less induction of the *speB* reporter, suggesting the possibility of some autoregulation (Fig. 2A). Reporter fluorescence examined by cytometry (Fig. 2B) and microscopy (Fig. S2B) were consistent with these observations. Similarly, the $\Delta speB$ and $\Delta covS$ mutants expressed slightly less, while $\Delta ropB$ bacteria expressed little (Fig. 2B, S2B).

Vfr is a dominant repressor for *speB*

Since secreted bacterial factors, including the SIP quorum-sensing peptide, give the potential for bacteria to coordinate expression within the population, we next performed media swap experiments. Wild-type *Spy* was grown to early exponential (EE), mid-late exponential (MLE), or stationary phase (SP) and the spent media removed, filtered, then used to supplement wild-type *Spy* growth carrying the SpeB reporter (Fig. 3A). As expected, since the SIP inducer accumulates in stationary phase cultures where SpeB is optimally expressed, SP spent media induced GFP (*speB*) (Fig. 3B). Surprisingly, however, growth from earlier growth phase cultures not only lacked *speB* inducer activity but suppressed its expression (Fig. 3B). This suggested that these cells produced a soluble factor that dominantly repressed the ability of other cells to produce SpeB. We next repeated the media swap experiment using a Δvfr mutant, which highly expressed SpeB (Fig. S2B), to see if a soluble factor from wild-type *Spy* could repress this. Spent media from only early-growth phase cultures could significantly repress this (Fig. 2B).

To assess whether it was Vfr itself in the media suppressing *speB*, we examined the activity of recombinant Vfr (rVfr). rVfr reduced GFP (*speB*) expression significantly in *Spy Δvfr (Fig. 3C). To assess the relative phenotypic dominance of SpeB regulation by autoregulatory mechanisms (Rop-SIP-Vfr dependent) versus environmental signaling mechanisms (CovRS-dependent), wild-type *Spy* containing the dual reporter was grown in the presence of CovRS inducers (LL-37 or MgCl₂) and Vfr at increasing concentrations. Both LL-37 and Vfr function synergistically in repressing *speB*, while Vfr antagonized MgCl₂-mediated induction of *speB* (Fig. 3D). Notably, *speB* expression in *Spy* Δvfr is unaffected by LL-37 or MgCl₂, further validating its dominance over CovRS regulation (Fig. S2C).*

Interestingly, the Vfr structure contains several potential protease SpeB cleavage sites (Fig. 3E)²². Since degradation could explain the SpeB-dependent changes in GFP (*speB*) expression, rVfr was incubated in the presence and absence of purified SpeB. Vfr degradation was observed in a concentration-dependent manner (Fig. 3F). Together, these data highlight that Vfr is a SpeB-labile repressor of SpeB expression.

speB is induced in the presence of immune effectors

Neutrophils are the first line of defense during innate immune response and are quickly recruited during bacterial infections. Neutrophils highly express the immune effector LL-37⁵, which *Spy* recognizes through CovRS, which by current models should repress *speB* expression. *Spy* grown with neutrophil lysates induced *hasABC* expression, consistent with CovRS stimulation, but did not repress *speB* expression (Fig. 4A). Similarly, in the mouse invasive infection model and in whole human blood, *Spy* induced *hasABC* while populations of high *speB* expressors were maintained (Fig. 4B). *Spy* with regulator knockouts were also evaluated to determine consistency in mouse and blood tissue infections with *in vitro* regulation. Δvfr maintained high *speB* expression, $\Delta ropB$ bacteria were negative for *speB* expression, and $\Delta covS$ contained a *hasABC* high population (Fig. S3A).

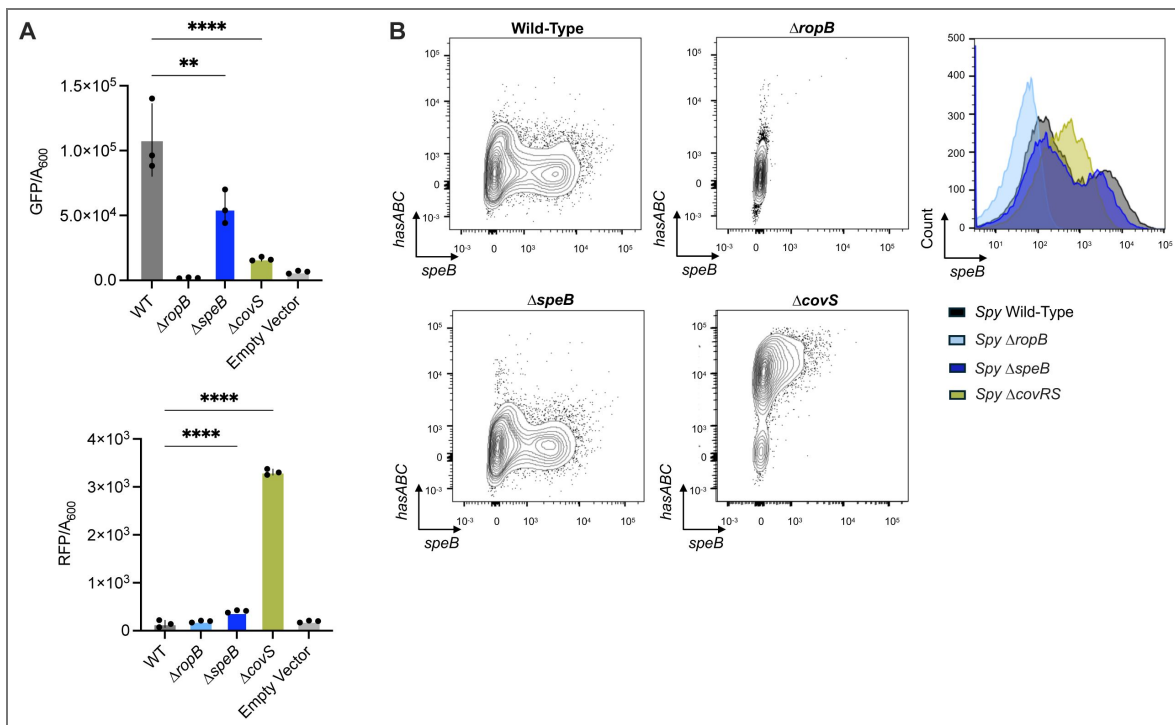


Fig. 2. *S. pyogenes* regulators are required for heterogeneous *speB* expression.

Spy genetic control strains of the *speB* regulatory circuit were evaluated. (A) Measurement of fluorescence over cell density after 10 h of growth. (B) Flow cytometry demonstrating *speB* expression (GFP; horizontal axis) and *hasABC* expression (RFP; vertical axis) of *Spy* growing at stationary phase. Statistical significance was determined using a one-way ANOVA with Dunnett's multiple comparisons test. *****P*<0.0001, ***P*<0.01, ns: not significant.

Fig. 3. Vfr is a dominant repressor for *speB*.

(A, B) Wild-type *Spy* was grown to early exponential (EE), mid-late exponential (MLE), and stationary phase (SP). Spent media from each stage of growth were collected and filter sterilized through 0.2µm filter and inoculated with *Spy* to detect GFP (*speB*) and RFP (*hasABC*) fluorescence. (C) *Spy* Δ *vfr* was grown in the presence or absence of recombinant Vfr (rVfr). (D) Wild-type *Spy* was grown with rVfr (0 - 10 µg/mL) and either LL-37 (0 - 300 nM) or MgCl₂ (0 - 15 mM) for 10 h. (E) AlphaFold structure of Vfr with potential *SpeB* cleavage sites (blue). (F) SDS-PAGE of Vfr (0.3 mg/mL) incubated with incremental concentrations of *SpeB* for 2.5 h. Statistical significance was determined using a one-way ANOVA with Dunnett's multiple comparisons test. ****P<0.0001, *P<0.05, ns: not significant.

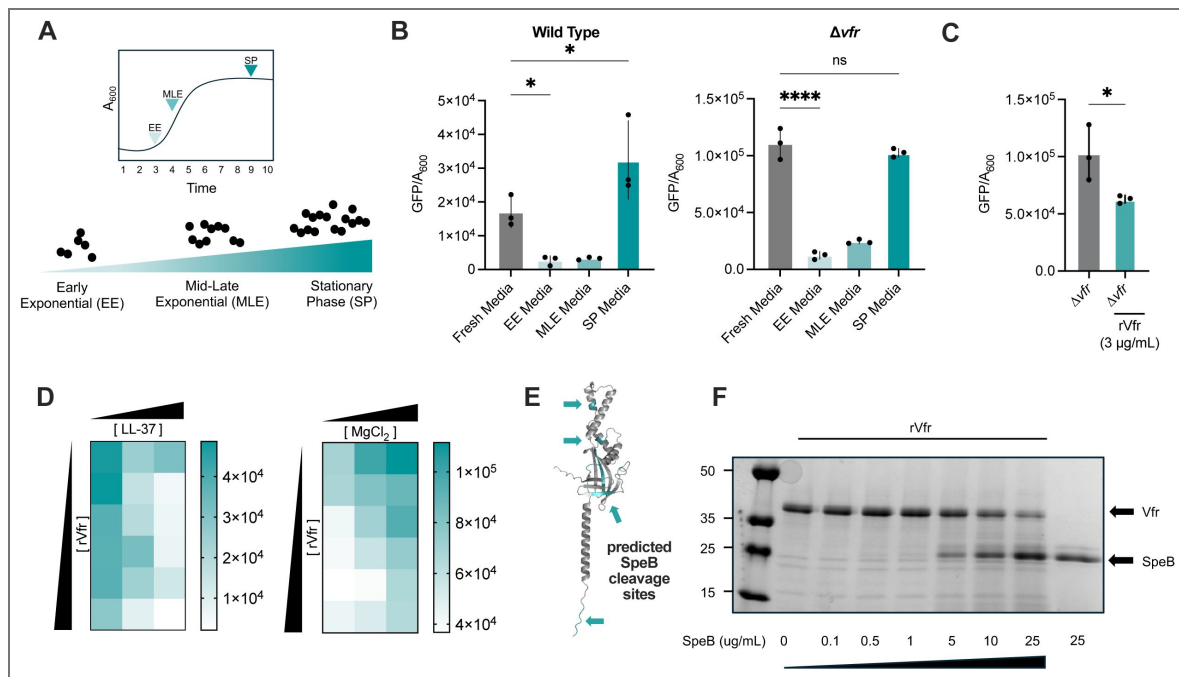
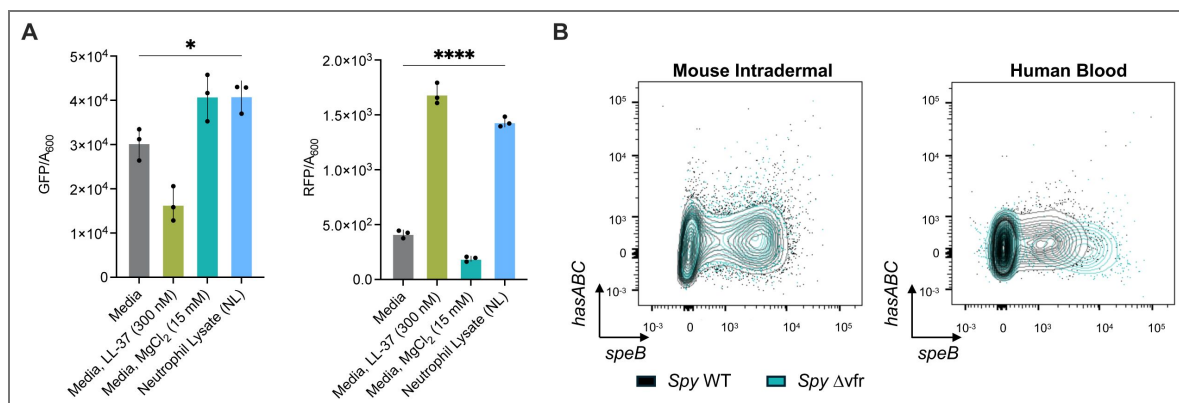


Fig. 4. *speB* expression is induced in the presence of immune effectors.

(A) Evaluating the effects of neutrophil lysate on *speB* and *hasABC* expression. *Spy* grew in the presence of neutrophil lysates (10⁶ cells/mL) compared to *Spy* growing in RPMI 5% THY. Treatment with LL-37 (300 nM) and MgCl₂ (15 mM) served as controls. (B) Flow cytometry demonstrating *speB* (GFP fluorescence; horizontal axis) and *hasABC* induction (RFP fluorescence; vertical axis) of 10⁸ CFU of *Spy* during mouse intradermal and human blood infections after 24 h and 4 h, respectively.



Immune effectors induce *speB* through Vfr

This high-level of expression *in vivo* suggested that *speB* could be induced, not just repressed, in the presence of immune effectors. Along with LL-37, neutrophil granules store many major inflammatory components secreted during infections^{23,24}. To assess whether other neutrophil derived molecules play a role in *speB* regulation, neutrophil lysates were fractionated and examined for their ability to induce or repress *speB* expression. Upon supplementation, GFP (*speB*) was induced by three fractions (10-12) containing active proteases (Fig. 5AB [↗](#)).

While *Spy* is resistant NET killing^{25,26}, the immune effectors released by neutrophils during NETosis, include not only LL-37, but proteases like neutrophil elastase (NE)²⁷. Based on the protease profile of NETs²⁸, Vfr contains several potential sites for cleavage (Fig. 5C [↗](#)). Neutrophils degraded rVfr (Fig. 5D [↗](#)), as did purified NE (Fig. 53C [↗](#)). The NE-specific inhibitor, BAY-678, was not sufficient to inhibit neutrophil lysate-mediated rVfr degradation, but serine inhibitors AEBSF and PMSF did (Fig. 5D [↗](#), 53C [↗](#)), suggesting a sufficiency but not requirement for other neutrophil proteases. Moreover, *Spy* grown with neutrophil lysates and inhibitor AEBSF had resulted in *speB* inhibition expression, compared to neutrophil lysate alone (Fig. 5E [↗](#)). Notably, these conditions maintained *hasABC* expression, consistent with CovRS stimulation (Fig. 53D [↗](#)). Altogether, these data suggest Vfr is a substrate for both bacterial and host-mediated degradation.

SpeB and neutrophils are sufficient to induce *speB* expression

To examine the impact that neutrophils have on *speB* regulation *in vivo*, neutrophils were depleted by anti-Ly6G treatment, as previously²⁹, significantly decreasing their numbers (Fig. S4A [↗](#)). After a 24 h intradermal infection, *Spy* from the tissue was examined by flow cytometry for *speB* expression, relative to a Δvfr control to define the high-expressing population (Fig. S4B [↗](#)). *Spy* expression of *speB* was only moderately decreased in the absence of neutrophils (Fig. 6B [↗](#)). However, infection of neutropenic mice with a $\Delta speB$, where there is neither host or microbial proteases to cleave Vfr, prevented *speB* expression (Fig. 6B [↗](#)). Mice deficient in peptidyl-arginine deiminase 4 (PAD4) are unable to form NETs³⁰. To separately examine NET contributions $PAD4^{-/-}$ mice were infected with *Spy* and *speB* expression examined. SpeB expression was reduced in $PAD4^{-/-}$ mice, additively with a contribution of SpeB itself (Fig. 6C [↗](#)). Collectively, this data suggests that *Spy* integrates the sensing of both neutrophils and feedback from SpeB to titrate expression during infection.

Discussion

Since a bacterium must adapt to environmental changes, they modulate expression in response to diverse stimuli, including stress, metabolites, quorum sensing, pH, and temperature. The niche of *Spy* is exclusively the human, potentially limiting its exposure to the range that some other species face. Yet within this host, it is nonetheless presented with challenges. Foremost amongst these are the immune defenses, which escalate through the course of infection. Fine-tuning its regulation toward the virulence factors needed to overcome this specific challenge is key to the species. SpeB is a potent pro-inflammatory virulence factor required to establish infection and has key roles in determining the course and severity of infections⁶. Accordingly, the regulation of SpeB must be tied to circumstances where it will be advantageous. Regulation of *speB* is thus multifactorial, as it integrates sensors to promote colonization and survival. In this study, we highlight a novel mechanism for SpeB regulation through Vfr detection of neutrophils and their activation state. Our data shows that neutrophils, despite functioning as an LL-37 reservoir expected to repress *speB* expression through the CovRS system, actually induces it during invasive skin infections.

The relative contributions of these regulators could vary by disease³¹. In response to inflammation, neutrophils are recruited to infection sites to engulf and inactivate pathogens. Despite neutrophils playing a major role in combating most infections, several studies indicate they can worsen *Spy* infections, in particular, in the upper respiratory tract^{29,32}. Here, RopB can detect the SIP homologs used for quorum sensing by other *Streptococci* species of the upper respiratory microbiota³³. This ensures SpeB expression at low cell densities and could allow SpeB

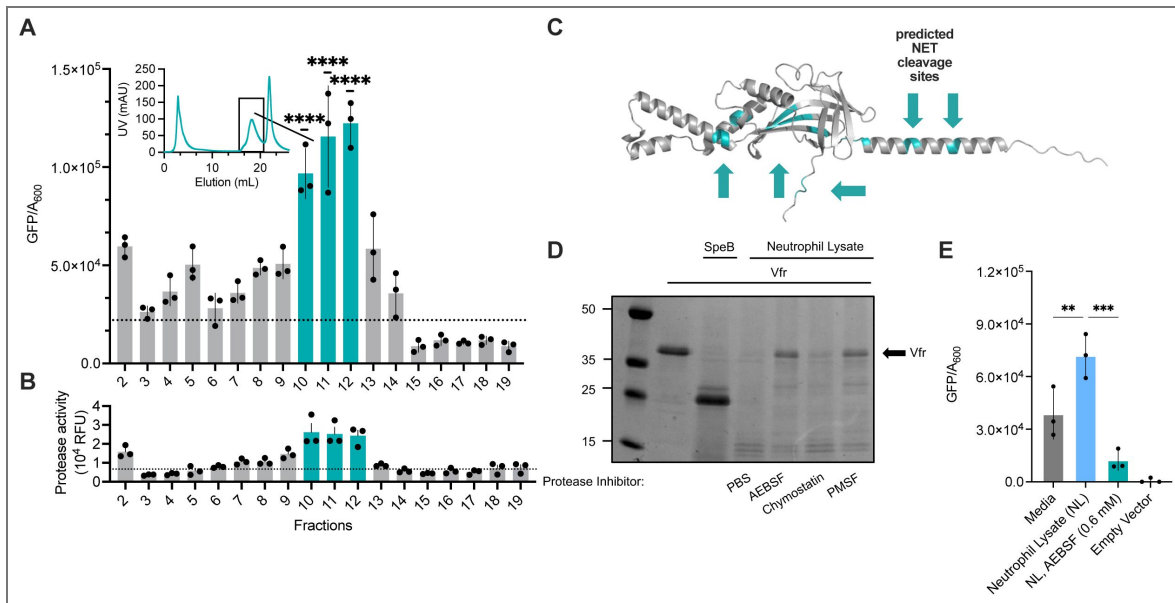


Fig. 5. Immune effectors induce *speB* through Vfr.

(A, B) Neutrophil lysates were fractionated based on net surface charge through anionic exchange. (A) Fractions were used to supplement *Spy* growth and *speB* expression was evaluated with GFP fluorescence at late log phase. Protein content within each elution (mL) was detected by UV (mAU) (Upper left). (B) Fractions were also used to evaluate protease activity. (C) AlphaFold structure of Vfr with potential NET protease cleavage sites (blue). (D) SDS-PAGE of Vfr (0.3 mg/mL) incubated with lysate from neutrophils (10^6 cells/mL) treated with inhibitors AEBSF, Chymostatin, or PMSF. PBS served as a vehicle control. (E) *Spy* grew in the presence of neutrophil lysates (10^6 cells/mL) and AEBSF (0.6 mM) compared to *Spy* growing in RPMI 5% THY. Statistical significance was determined using a one-way ANOVA with Dunnett’s multiple comparisons test. **** $P < 0.0001$, *** $P < 0.001$, ** $P < 0.01$.

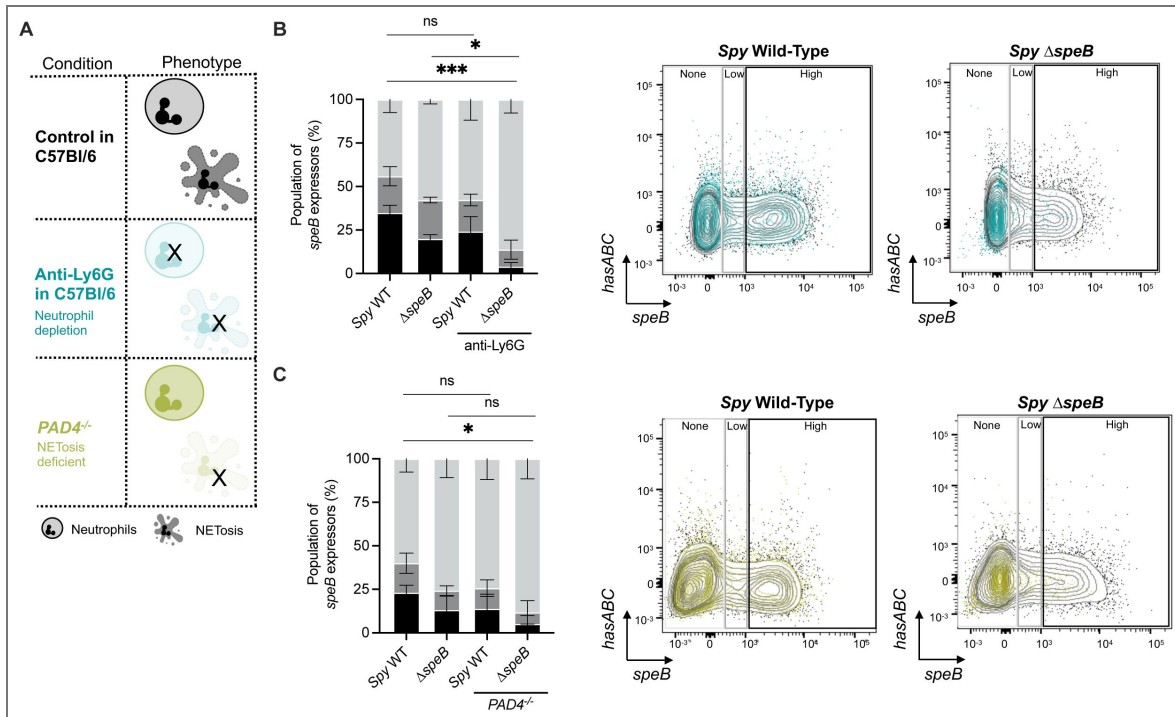


Fig. 6. SpeB and neutrophils are sufficient to induce *speB* expression.

(A) Diagram of mouse intradermal infection model in three different conditions: neutrophil-depleted mouse (anti-Ly6G treatment); NET-deficient mouse (*PAD4*^{-/-}); and neutrophil competent (wild-type) control. (B, C) Flow cytometry on mouse skin lesions from 24 h intradermal infection of 10⁸ CFU of *Spy* or *Spy* Δ*speB*. Population of *speB* expressors was determined based on fluorescent intensity during flow cytometry. No expressors range was based on the negative empty vector control. (B) C57Bl/6 mice were treated with neutrophil-depleting antibody, anti-Ly6G, (blue) or control (black) for 24 h then infected. (C) NETosis-deficient mice (*PAD4*^{-/-}, yellow) or control (C57Bl/6 mice, black) were infected. Statistical significance of high *speB* expressors was determined using a two-way ANOVA with Dunnett's multiple comparisons test. ***P<0.001, *P<0.05, ns: not significant.

expression even before neutrophil infiltration. Importantly, the type of CovS mutants that interfere with SpeB expression do not occur during human pharyngitis or experimental mouse models of it, and $\Delta speB$ mutants are highly attenuated, indicating its essentiality at this site²⁹. This would subsequently require SpeB expression during infections, suggesting repression by LL-37, released by the abundant neutrophils recruited during infection, is, at best, limited.

Our work suggests that Vfr functions as a biosensor of protease activity that regulates the major protease of *Spy*, SpeB. It is additionally degraded by neutrophil proteases, thereby relieving repression in the presence of these important immune cells. Originally identified through a transposon mutagenesis screen¹⁸, Vfr has been suspected to regulate SpeB in a RopB-dependent manner¹⁹. Our results showing that Vfr functions as a negative regulator of *speB* early during growth in culture is consistent with this, but the mechanism in which SIP quorum sensing relieves Vfr-mediated repression at late and stationary growth remains to be elucidated. Since the SpeB protease itself can degrade Vfr, autoregulation may play a role in this temporal regulation. However, it is not clear whether this would be relevant during infection, since the host can provide the proteases to overcome this. Similarly, CovRS mediates repression of SpeB in some *in vitro* conditions, such as with LL-37 alone. However, since repression is not maintained in the presence of the major LL-37-producing cells, neutrophils, the effect may be more limited during infections, either due to heterogeneity in the population or dominant effects of Vfr. Importantly, other than releasing LL-37, neutrophils undergoing NETosis or degranulating release proteases, including NE³⁴, that degrade Vfr. Together, this highlights the importance of *in vivo* data for examining pathways such as the regulation of SpeB, since pathways sensing multiple bacterial and host factors can intersect.

In summary, we demonstrate how *Spy* overcomes challenges in the temporal regulation of the virulence factor SpeB by a circuit that integrates multiple considerations in the host-pathogen interactions. Clear Vfr homologues can be found throughout the Streptococci (*S. agalactiae*, *S. urinalis*, *S. pseudoporcinus*, *S. porcinus*, *S. uberis*, *S. iniae*, *S. equi*, *S. dysgalactiae*, *S. canis*), despite none of these species encoding a SpeB homolog. This suggests that Vfr may be a regulator module more generally, and that through these other species senses broader factors as well. We propose a model wherein *Spy*, through the Vfr protein, coordinates expression of SpeB within the bacterial population. At high cell densities, quorum sensing is sufficient to induce expression. However, Vfr allows expression at lower cell densities if there is sufficient protease to degrade it. This can be accomplished if there are some SpeB-expressing cells already, thus leading to further coordination between cells independent of classic quorum-sensing, or, an override in the instance of proximate protease-producing immune cells. This further allows heterogeneity within the population, as each cell is exposed to different concentrations of SIP, LL-37, VFR, and protease. Altogether, beyond demonstrating a previously undescribed mechanism for regulating a protease through a natural biosensor for its activity, we show that this integrated regulation poises the pathogen to respond to shifts in innate immune pressure as part of the sophisticated virulence strategy of *Spy*.

Methods

Bacterial strains and growth conditions

All strains are described in Table 1 [↗](#). *Spy* strains were routinely grown in Todd Hewitt broth with 5% yeast (THY) at 37°C with 5% CO₂. Bacterial aliquots were washed in PBS and resuspended in PBS with 20% glycerol for storage at -80°C and grown fresh for each experiment. The bacterial mutations $\Delta covS$, $\Delta ropB$, and Δvfr were obtained through lambda red recombineering, as described previously³⁹. Briefly, a kanamycin resistance cassette was PCR amplified with the primer sequences outlined in Table 2 [↗](#), each carrying 5' homology to the chromosomal sequence flanking the sites of the desired mutation. *Spy* 5448 carrying recombineering plasmid pAV488 were electroporated with the PCR product and selected for kanamycin resistance. Curing of the recombineering plasmid was achieved by selecting colonies susceptible to chloramphenicol. Gene knockout and lack of spurious secondary-site mutations were validated by whole-genome sequencing (Plasmidsaurus). Reference sequences and plasmids are detailed in Table 3 [↗](#).

<i>S. pyogenes</i> strain	Description	Reference
M1 5448	Wild-type M1	Ref ³⁵
5448ΔcovR	Deletion of <i>covR</i>	This study
5448ΔcovS	Deletion of <i>covS</i>	This study
5448ΔropB	Deletion of <i>ropB</i>	This study
5448ΔspeB	Deletion of <i>speB</i>	Ref ³⁶
5448Δvfr	Deletion of <i>vfr</i>	This study

Table 1. Strain List

Plasmid name	Description	Reference
pDCerm	Reporter backbone	Ref ³⁷
pGFP	Plasmid with <i>gfp</i> template	GenBank: OM212390.1
pRFP	Plasmid with <i>rfp</i> template	GenBank: KM521211.1
pDCerm GFP	Reporter construct	This study
pDCerm mCherry	Reporter construct	This study
pDCerm-PspeB::GFP	<i>speB</i> expression reporter	This study
pDCerm-PhasA-mCherry	<i>hasA</i> expression reporter	This study
pDCerm-PspeB::GFP-PhasA::mCherry	Dual <i>speB</i> and <i>hasA</i> expression reporter	This study
pET-SUMO	Expression vector	Ref ³⁸
pET-SUMO Vfr	Vfr expression vector	This study
pAV488	Recombineering plasmid	Ref ³⁹

Table 3. Plasmids

Plasmids

Fluorescent reporter plasmids pDCerm-*PspeB::GFP*, pDCerm-*PhasA::RFP*, and pDCerm-*PspeB::GFP-PhasA::RFP* were created for this study by Polymerase Incomplete Primer Extension (PIPE) cloning technique, as previously described⁴⁰. *Spy* promoters were amplified from 5448, GFP from (GenBank: OM212390.1), and RFP from (GenBank: KM521211.1) for insertion into pDCerm⁴¹ using the primers in Table 2⁴². The sequence was validated using whole plasmid sequencing (Plasmidsaurus) and constructs transformed into each *Spy* strain by electroporation. Expression vector pETxSUMO-Vfr was created using primers Vfr F and Vfr R to amplify *vfr* from GAS 5448 and the previously described PIPE primers pETxSUMO F and pETxSUMO R to amplify the expression vector⁴⁰. Reference sequences and plasmids are detailed in Table 3⁴³.

Fluorescence during growth

Spy 5448 strains grown in Todd-Hewitt Broth with 5% yeast (THY) to mid-exponential phase were used to inoculate fresh, phenol red-free RPMI supplemented with THY (5%) and erythromycin (2 μg/mL) in a 96-well black, clear-bottom plate (Costar). Cultures were grown for 10 hours at 37 °C and 5% CO₂ with measurements of absorbance (600 nm), GFP (ex. 479 nm, em. 520 nm), and RFP (ex. 579 nm, em. 616 nm) using a BioTek Synergy H1 plate reader. Expression of *speB* and *hasABC* were analyzed by fluorescence of GFP or RFP over absorbance. Supplementation with LL-37 300 nM (GeneScript) and MgCl₂ 15 mM (Sigma M9272).

Whole blood and neutrophil experiments

Whole blood was collected from healthy adult donors with informed consent and approval from the Emory University's Children's Clinical and Translational Discovery Core. For infections, 10⁸ CFU bacteria suspended in 100 μL of PBS and used to inoculate 400 μL of whole blood. Inoculated blood was incubated on a rotisserie mixer for 4 h. After 4 h, to lyse host cells, the inoculum was treated with Triton X 0.05% (Sigma T8787) for 15 minutes, then samples were stained and fixed for

Table 2. Cloning Primers Primer

Primer name	Application	Sequence
pDCerm_GFP A	GFP construct on pDC::erm backbone	5'- ctaatgttgtaatgtaataaggtATGAGTAAAGGAGAAGAACCTTTTC A
pDCerm_GFP B	GFP construct on pDC::erm backbone	5'- gaggaacaaggaaatgaagCTATTTGTATAGTTTCATCCATGC
pDCerm_RF P A	RFP construct on pDC::erm backbone	5'- ctaatgttgtaatgtaataaggtATGGTTTCAAAGGTGAAGAA GA
pDCerm_RF P B	RFP construct on pDC::erm backbone	5'- gaggaacaaggaaatgaagCTATTTGTAAAGTTCATCCATAC CA
pDCerm_GFP/RF P C	GFP/RFP construct on pDC::erm backbone	5' - accttalttaacattcacaacattag
pDCerm_GFP/RF P D	GFP/RFP construct on pDC::erm backbone	5' - ettcatttcctgtttcctcctag
PspeB-GFP A	PspeB controlled GFP on pDC::erm backbone	5' - ctaatgttgtaatgtaataacaagccttctagttg
PspeB-GFP B	PspeB controlled GFP on pDC::erm backbone	5' -gaaaagttcttctctttactcattttttatacctc
PspeB-GFP C	PspeB controlled GFP on pDC::erm backbone	5' -ttattaacattcacaacattagcgg
PspeB-GFP D	PspeB controlled GFP on pDC::erm backbone	5' -atgagtaaaggagaagaactttc
PhasA-RFP A	PhasA controlled RFP on pDC::erm backbone	5'- ctaatgttgtaatgtaataatcagatgaagtgt
PhasA-RFP B	PhasA controlled RFP on pDC::erm backbone	5'-ttcttcacctttgaaaccataattacacctttctt
PhasA-RFP C	PhasA controlled RFP on pDC::erm backbone	5' -ttattaacattcacaacattagcgg
PhasA-RFP D	PhasA controlled RFP on pDC::erm backbone	5' -atggtttcaaaaggtgaagaa
PspeB_PhasA A	Dual GFP and RFP Reporter Construct	5' -ttgcattacctgacggaGATATCTAGAGCTCCGCGG
PspeB_PhasA B	Dual GFP and RFP Reporter Construct	5' -gcagtgacagagtacgctCGCTAGGAGGAAACAAGGA

Table 2. (continued)

PspeB_PhasA C	Dual GFP and RFP Reporter Construct	5' -tccgtcaggtaatgcaaa
PspeB_PhasA D	Dual GFP and RFP Reporter Construct	5' -agcgtactctgtcactgc
Δ covS F	<i>covS</i> deletion construct	5' - TTGTACAAAAACGATAAAACACATCTGAGAATTGATGAC AGAAAGGGCAGTCGAGTCATTAGGAGTGAGCGCGAT GATCCTCGAGCTCTAGATCTTAAGC
Δ covS R	<i>covS</i> deletion construct	5' - AGCCTGGTACTTGTTCGATTACGTGATTATCCGTTCTAT AAAAGCGTTCAAAGATATGTCCATGGCGCGTTACCAAT TAG
Δ covR F	<i>covR</i> deletion construct	5' - ACTGCTTTGGAAAAAGAGTTTGATTAAATCCTGCTTG ACTTAATGTTACCAGAGATGGATGGTTTTGAAGGATC CTCGAGCTCTAGATCTTAAGC
Δ covR R	<i>covR</i> deletion construct	5' - CACTGTTTGATATAAGATTCCTTGCCCTGGAATGTCA ATTTGCGCGGAGATAACGAATATAGACATCTCATG GCGCGTTACCAATTAG
Δ ropB F	<i>ropB</i> deletion construct	5' - AACCGTTGAATTCATTAGGCATTCAAAAAACATTCGATT AAACAAGTTTGTGGTGATTATCTCACTAGGCAAACGATCC TCGAGCTCTAGATCTTAAGC
Δ ropB R	<i>ropB</i> deletion construct	5' - TCAGGACAGTTTATGTTAATGGCTTCTAGGTAGGTTTGA AACATATGATGGATCGTTTTGCAATTAAGTAATTGCATGG CGCGTTACCAATTAG
Δ vfr F	<i>vfr</i> deletion construct	5' - TCATAGTTAGGTTTACCGATTTACTTGACGCCTAAT GATGACATGCTAGTATTTTATTAAGGAGATGAGTC GATCCTCGAGCTCTAGATCTTAAGC
Δ vfr R	<i>vfr</i> deletion construct	5' - AAACTTCTCAATTGAATAATTTTCAAACATGAAAA AATCCGTCTGTGACTACGTTATACACTGACGGACTT CATGGCGCGTTACCAATTAG
pET-SUMO-vfr-F	<i>vfr</i> expression plasmid	CTCACAGAGAACAGATTGGTGGTATGACACAAGTAGCCC AAGG
pET-SUMO-vfr-R	<i>vfr</i> expression plasmid	TGCTCGAGTGCGGCCTCA GAGTAATCCTTTTGAAAAAGAAGTATGTC

analysis. For neutrophil experiments, neutrophils were isolated from whole human blood by centrifugation in PolymorphPrep (AxisShield) as previously⁴², then diluted in RPMI. To obtain protein content from neutrophils, suspension with neutrophils in RPMI were lysed via sonication (11% amplitude for 4 minutes at 30 second intervals) and centrifuged at 6,000 x g for 5 minutes to remove cellular debris. Neutrophil lysates were used for plate reader analysis or SDS PAGE. Serine protease inhibitor AEBSF 0.6 mM (Sigma 508436) was used for plate reader analysis.

Animal experiments

All animal use and procedures were performed with approval from Emory Institutional Animal Care and Use Committee. Mice were housed in specific pathogen-free conditions with a 14 h light/10 h dark cycle in a standard ambient environment (~20 °C and ~50% humidity) in ABSL-2 conditions. Experiments were performed using both male and female wild-type C57Bl/6 and NET-deficient *PADA*^{-/-} (JAX #030315)³⁰ mice of 8-12 weeks of age (Jackson Laboratories). There was no attrition or drop out of subjects. Animal were assigned to experimental groups using simple randomization. In experiments where neutrophils were depleted, 50 µg anti-Ly6G (1A8) (BioXCell) or PBS vehicle control were delivered intraperitoneally 24 h before infection. Depletion was confirmed by flow cytometry using Ly6G (Invitrogen 367-9668-82), CD11b (Invitrogen 63-0112-82), and CXCR1 (RD Systems FAB8628P) antibodies as previously²⁹. *Spy* 10⁸ CFU were suspended in 100 µL of PBS and injected subcutaneously, as previously³⁸. After 24 h, mice were euthanized, lesions excised and mechanically homogenized, then stained and fixed for analysis.

Flow Cytometry

All samples were pelleted at 12,000 x g and washed with PBS with 1 mM EDTA. For viability, samples were stained using BactoView™ Dead 760/780 (Biotium cat. 40113) as per manufacturer protocol, then strained through a 100 µm filter (Avantor). Samples were fixed using 4% paraformaldehyde for 30 minutes. To stain for Group A Carbohydrate (GAC), unique to *Spy*, samples were incubated with goat anti-GAC antibody (Fitzgerald 70-XG70_R) for 1 hour, then rabbit anti-goat APC (Invitrogen A56570) for 1 hour. Samples were analyzed using BD FACSymphony A3 with excitation lasers: FITC, PE-594-A, APC, APC-Cy7. Appropriate single-color controls were used as compensation controls for these experiments. Data was analyzed using FlowJo, *RRID:SCR_008520* <https://doi.org/10.1002/scr.008520>. For analysis, *speB* expressors were determined based on fluorescent intensity. Non-expressors were determined by background fluorescence from the *Spy* empty vector negative control, below 10². Low expressors were identified between the ranges of 10² and 10³, whereas high expressors were identified above 10³.

Protein expression and purification

Expression plasmid pETxSUMO-Vfr was introduced to *Escherichia coli* Rosetta (DE3) and induced at 37°C for 3 hour with 1 mM isopropyl-β-D-thiogalactopyranoside (IPTG) when O.D. 600 reached 0.4-0.6. Cells were pelleted resuspended in buffer (20 mM Tris-HCl pH 8.0) and disrupted with sonication. Lysates were centrifuged at 20,000 x g 10 minutes at 4°C. Inclusion bodies were washed twice with wash buffer 1 (20 mM Tris-HCl, 2 M urea, 0.3 M NaCl, 2% TritonX-100 pH 8.0) and dissolved in binding buffer (20 mM Tris-HCl, 0.5 M NaCl, 5 mM imidazole, 6 M guanidine hydrochloride, 1 mM 2-mercaptoethanol pH 8.0). Sample was mixed at low speed for 40 minutes at room temperature and then filter-sterilized through 0.22 µm filter (Avantor). Filtered sample was loaded to a washed and equilibrated HisTrap HP column (Cytivia) with 0.5 ml NiSO₄. Sample within the column was washed with binding buffer and wash buffer 2 (20 mM Tris-HCl, 0.5 M NaCl, 6 M urea, 1 mM 2-mercaptoethanol pH 8.0). Refolding was performed with FPLC (AKTA start) using a urea linear gradient up to 6 M urea. Gradient volume was 30 mL and flow rate was 1 mL/minute. Sample was eluted using an imidazole linear gradient up to 400 mM imidazole in elution buffer (20 mM Tris-HCl, 0.5 M NaCl, 400 mM imidazole, 1 mM 2-mercaptoethanol pH 8.0). Gradient volume was 10 mL and flow rate was 0.5 mL/minute. Fractions containing eluted protein were pooled and quantified. SpeB was purified as previously described^{38,43}.

Vfr Cleavage Assay

For *in vitro* cleavage experiments, recombinant Vfr (rVfr) (0.3 mg/mL) was incubated with titrations of purified SpeB (0.1 - 25 µg/mL) or recombinant Neutrophil Elastase (1 µg/mL; Sigma 324681) in assay buffer (Tris 25 mM, 300 mM NaCl, 2 mM dithiothreitol) at 37°C for 2 hours. Proteins and their cleavage products were then separated by SDS-PAGE and visualized by AcquaStain (Bulldog Bio). For neutrophil protein cleavage, purified rVfr (0.3 mg/mL) was incubated with neutrophil soluble protein (as described above) from 10⁶ cells/mL in RPMI supplemented with 2 mM dithiothreitol for 12 hours. Protease inhibitors AEBSE, Chymostatin, and PMSF were used as per manufacture protocol (G Biosciences 786-207). Neutrophil Elastase selective protease inhibitor BAY-687 (Cayman 18615) was used in titrating quantities (0.1 - 20 µg/mL).

Protein Modeling and Cleavage Prediction

The structure of Vfr was modeled as a dimer in AlphaFold Server v3 and visualized in PyMOL, *RRID:SCR_000305* [↗](#). Sites of potential SpeB cleavage were predicted as previously described based on known targets⁴⁴ using ScanProsite (Expasy) with a search for the motif [IVFYM]-[ADEGKSTN] and the included condition for a net negative charge sidechain charge in the P1'-P5' region. Sites of NET cleavage are from the motif previously described²⁸.

Protein Fractionation

Neutrophils isolated from whole blood (as above) were pelleted at 2,000 x g for 5 minutes and washed in Tris 20 mM, 1 M NaCl pH 8.0, then disrupted with sonication on ice. Neutrophil lysate was centrifuged at 20,000 x g at 4°C and filter sterilized through 0.22 µm filter (Avantor) then separated by anionic exchange by FPLC (Cytiva). Neutrophil protein was fractionated with a linear NaCl gradient up to 1 M NaCl in 20 mM of Tris. Fractions were assessed by SDS-PAGE and assayed with *Spy* containing GFP (*PspeB::gfp*) fluorescent reporter.

Protease activity

Internally-quenched FRET peptides IFFDTWDNE, TWDNEAYVH, EAYVHDAPV, and HDAPVRSLN that detect neutrophil proteases⁴⁵ were pooled (2.5 µM each) in PBS, 1 mM CaCl₂, 0.01% Tween-20 (Sigma P7949) and unincubated with each column fraction. After 1 hour incubation at 37°C, the proteolysis was measured using an Nivo plate reader (PerkinElmer) with fluorophore excitation at 323 nm and emission at 398 nm as previously⁴⁵. Measurements of SpeB activity within bacterial supernatants was performed as previously with the fluorescent peptide sub103, internally quenched with an N-terminal Mca and the C-terminal Lys-Dnp (CPC Scientific)⁴³. In triplicate, 10 µM of peptide was incubated in assay buffer (PBS with 2 mM dithiothreitol) with 10 µL of supernatant at 37°C for 30 minutes. Kinetic fluorescence was measured every 30 sec (ex. 323 nm, em. 398 nm) using a Victor Nivo plate reader (PerkinElmer).

Statistics

GraphPad Prism, *RRID:SCR_002798* [↗](#), was used to evaluate statistical significance. Unless otherwise stated, one-way ANOVA with Dunnett's multiple comparisons test was used for the statistical analysis of experiments and P values < 0.05 were considered significant.

Data availability

All supporting data have been supplied with the manuscript.

Supplementary Figures

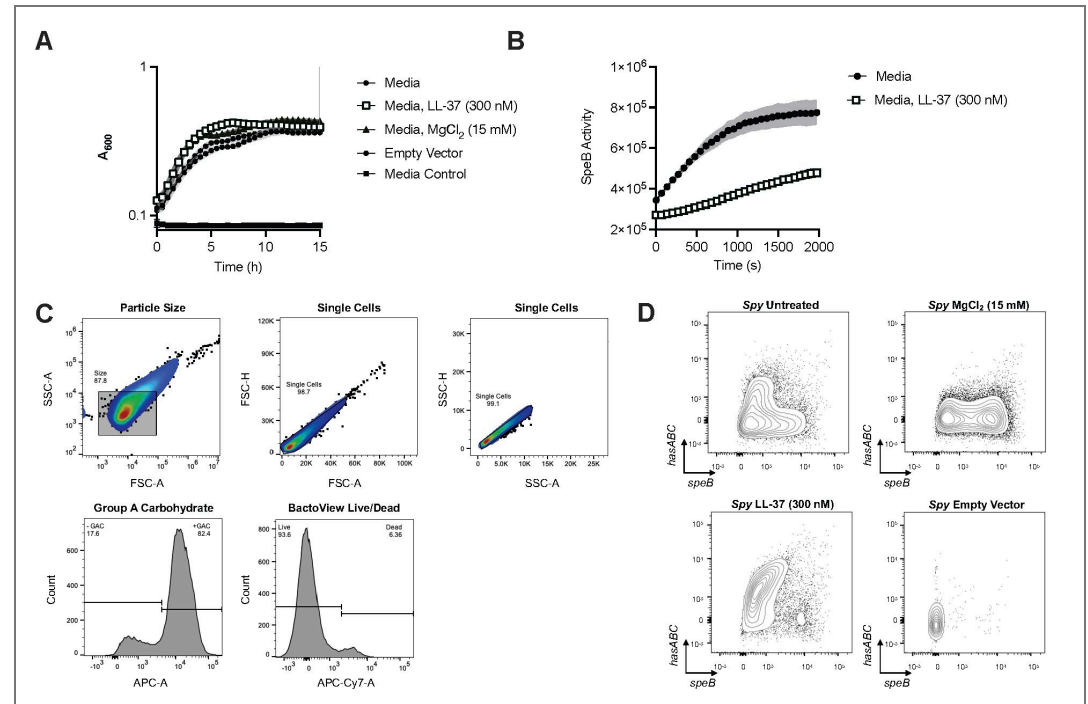


Fig. S1. (A) Wild-type *Spy* growth kinetics determined through optical density at 600 nm (O.D. 600) in RPMI, 5% THY with LL-37 (300 nM) or $MgCl_2$ (15 mM). (B) SpeB activity was measured using the fluorescent peptide sub103. (C) Flow cytometry gating strategy for measuring *Spy* GFP and RFP fluorescence. Samples were selected based on particle size (FSC-Area, SSC-Area), then selected for into single cells (FSC-Area, Height; SSC-Area, Height). Sample containing Group A Carbohydrate (APC-A positive population; right peak) were selected. Lastly, live cell population was selected (APC-Cy7-A negative population; left peak). (D) Flow cytometry demonstrating *speB* expression (GFP; horizontal axis) and *hasABC* expression (RFP; vertical axis) of *Spy* growing at stationary phase separated in panels based on treatment.

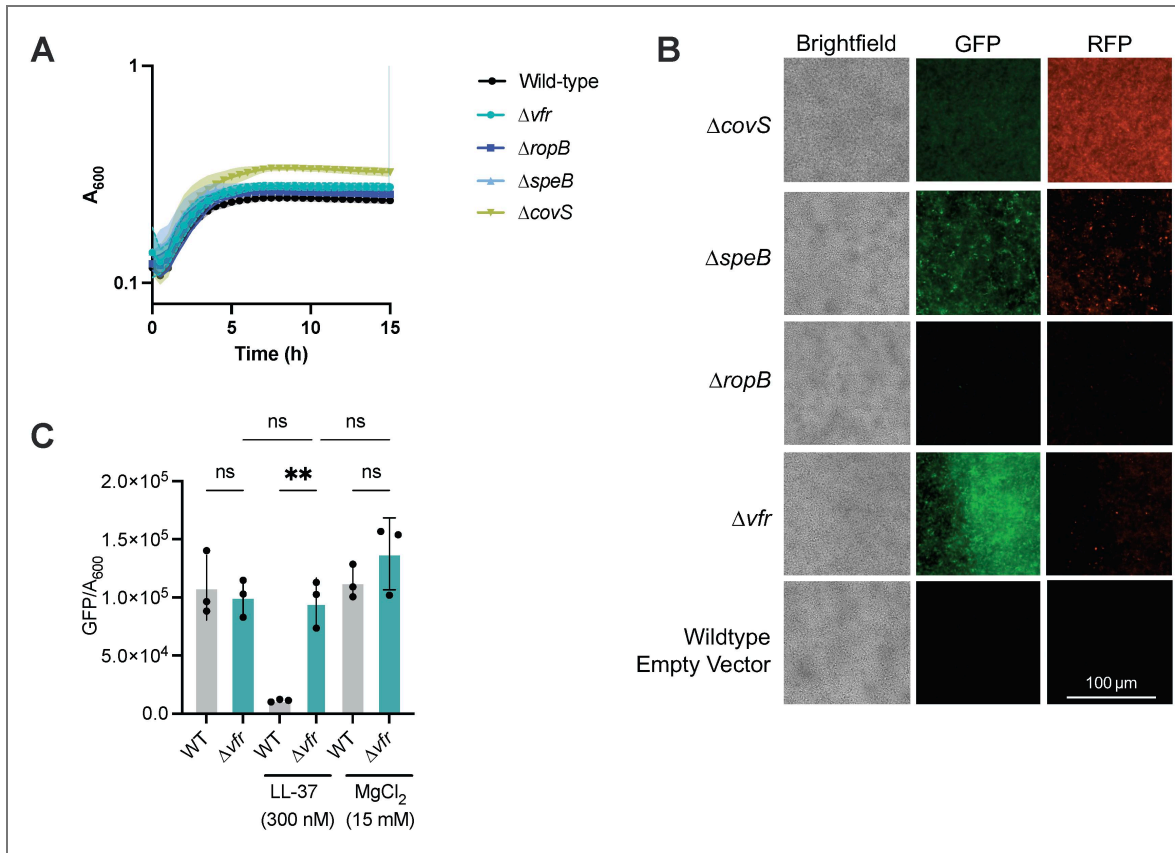


Fig. S2.

(A) *Spy* growth kinetics determined through optical density at 600 nm (O.D. 600) in RPMI, 5% THY. (B) Lionheart live-cell fluorescent microscopy with brightfield, GFP, and RFP channels on of *Spy* culture grown at stationary phase. Scale bars, 100 μm . (C) Measurement of fluorescence over cell density after 10 h of growth. Wild-type and Δvfr *Spy* were treated with LL-37 (300 nM) or MgCl₂ (15 mM).

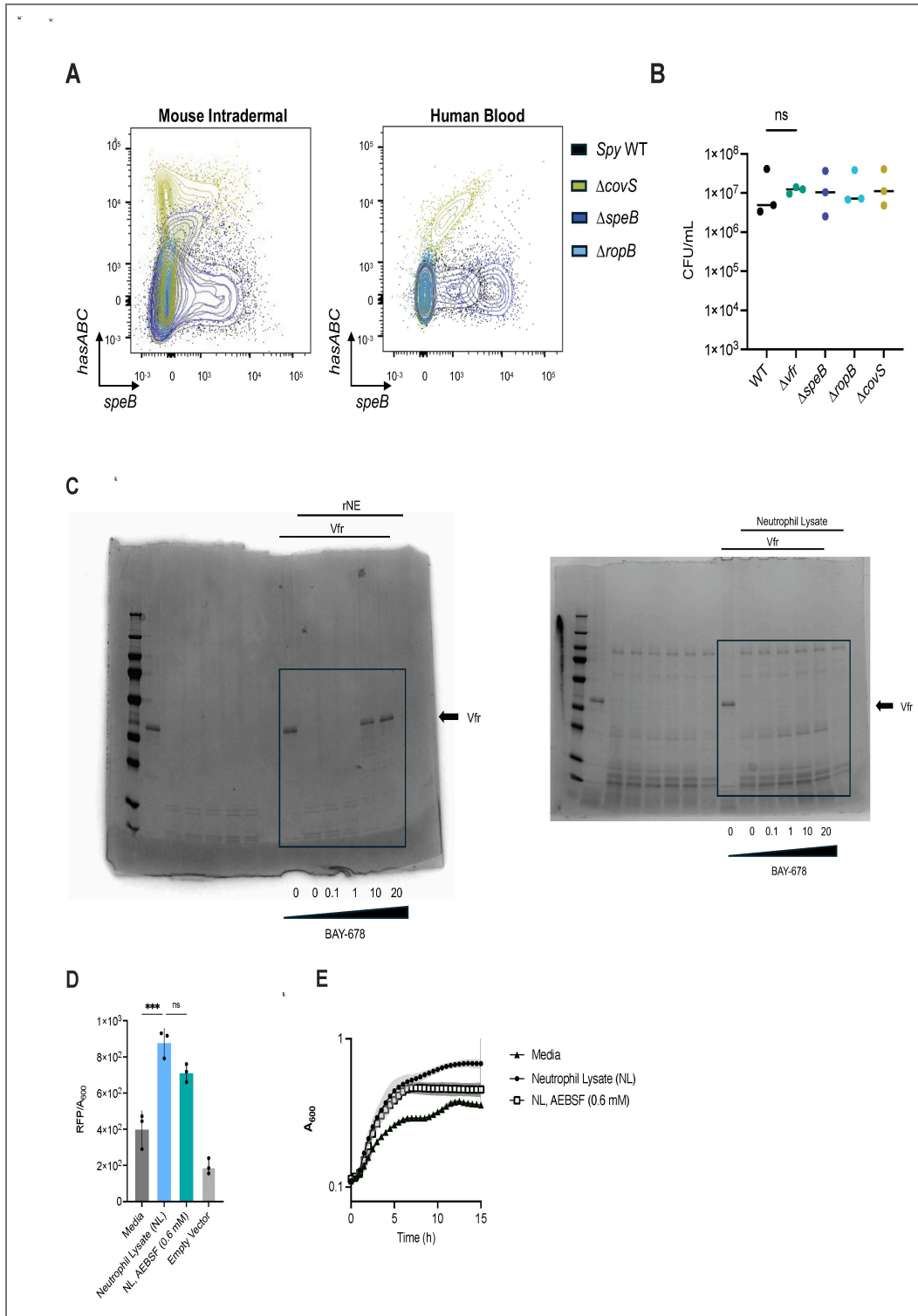


Fig. S3.

(A) Regulation of *speB* and *hasABC* during mouse intradermal and human blood infections. Flow cytometry demonstrating *speB* (GFP fluorescence; horizontal axis) and *hasABC* induction (RFP fluorescence; vertical axis) of 10^8 CFU of *Spy* strains. (B) Colony Forming Units (CFU) of *Spy* within 4 h human blood infection was measured by plating. (C) SDS-PAGE of Vfr (0.3 mg/mL) incubated with recombinant Neutrophil Elastase (rNE) or neutrophil lysate (10^6 cells/mL) with inhibitor BAY-678. (D) Measurement of RFP fluorescence (*hasABC*) over cell density after 10 h of growth. (E) *Spy* growth kinetics determined through optical density at 600 nm (O.D. 600).

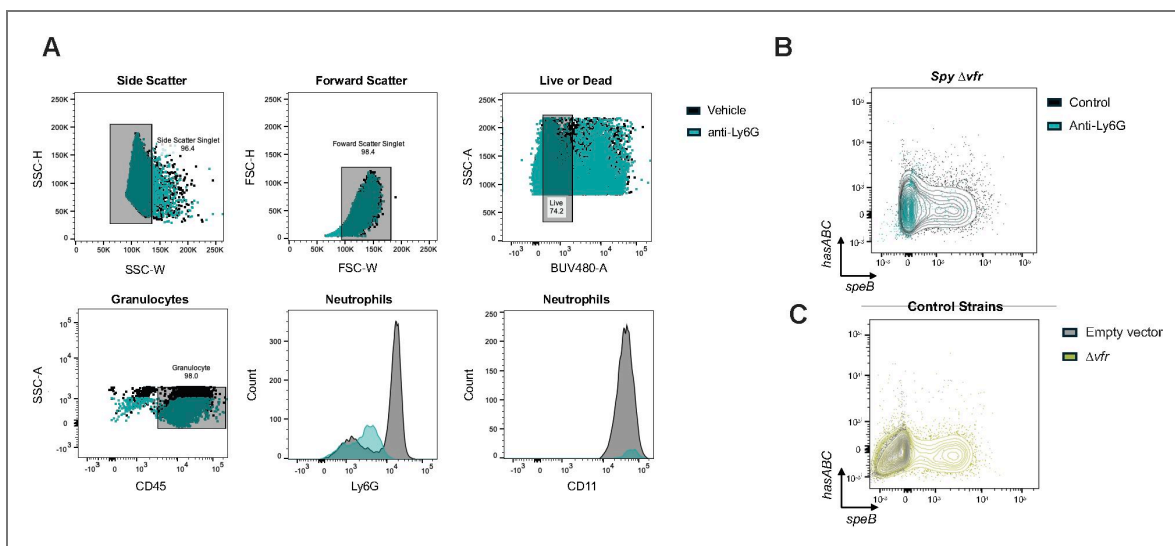


Fig. S4.

(A) Flow cytometry gating strategy for neutrophil depletion model with anti-Ly6G. Singlets were selected through side (SSC-H, SSC-W) and forward (FSC-H, FSC-W) scatter. Population of live cells were selected based on BUV480-A fluorescence (left). Granulocytes were selected based on the presence of CD45, and neutrophils were identified based on presence of Ly6G and CD11. (B, C) Flow cytometry demonstrating *speB* (GFP fluorescence; horizontal axis) and *hasABC* induction (RFP fluorescence; vertical axis) of 10^8 CFU of *Spy*. *SpyΔvfr* strain in anti-Ly6G neutrophil depletion model (B). Control strains, *Spy* empty vector and *Δvfr*, during mouse intradermal infection with *PAD4*^{-/-} (C).

Acknowledgements

We thank Victor Nizet and Andrew Varble for strains, the anonymous blood donors, and members of LaRock lab for helpful discussions. This work was supported in part by the Emory University Integrated Cellular Imaging Core Facility (*RRID:SCR_023534* [↗](#)), the Emory Flow Cytometry Core (EFCC) Facility (*RRID:SCR_023536* [↗](#)), and the Children's Healthcare of Atlanta and Emory University's Children's Clinical and Translational Discovery Core. Additional support was provided by the National Center for Georgia Clinical & Translational Science Alliance of the National Institutes of Health under Award Number UL1TR002378. This work was supported by the National Institute of Allergy and Infectious Diseases of the NIH under award numbers AI153071 (C.N.L.) and AI180089 (C.N.L.), training grants AI106699 (S.G.), AI179103 (S.G.), an American Heart Association Predoctoral Fellowship 25PRE1372818 (A.D.), and a Burroughs Wellcome Fund Investigator in the Pathogenesis of Infectious Disease award (C.N.L.). The content is solely the responsibility of the authors and does not necessarily reflect the official views of the National Institutes of Health.

Additional information

Author Contributions

Conceptualization, C.N.L.; investigation and analysis, S.G., A.D., D.L.L., C.N.L.; writing of the original draft, S.G. and C.N.L.; reviewing and editing, S.G. and C.N.L.; funding, S.G., A.D., C.N.L.; supervision, C.N.L.

Funding

Funder	Grant reference number	Author
HHS NIH National Institute of Allergy and Infectious Diseases (NIAID)	AI153071	Christopher LaRock
HHS NIH National Institute of Allergy and Infectious Diseases (NIAID)	AI180089	Christopher LaRock
HHS NIH National Institute of Allergy and Infectious Diseases (NIAID)	AI106699	Stephanie Guerra
HHS NIH National Institute of Allergy and Infectious Diseases (NIAID)	AI179103	Stephanie Guerra
American Heart Association (AHA)	https://doi.org/10.58275/aha.25pre1372818.pc.gr.227140	Ananya Dash
Burroughs Wellcome Fund (BWF)	Investigator in the Pathogenesis of Infectious Disease	Christopher LaRock

Author ORCID iDs

Christopher N LaRock:  <https://orcid.org/0000-0003-3035-5331>

Additional files

Supplementary file 1. [↗](#) Fill size gels from primary figures.

Supplementary file 2. [↗](#) Raw data for Figures 1-6.

Supplementary file 3. [↗](#) Raw data for Supplemental Figures.

References

1. Carapetis JR, Steer AC, Mulholland EK, Weber M (2005) The global burden of group A streptococcal diseases. *Lancet Infect Dis* **5**:685-694 [https://doi.org/10.1016/s1473-3099\(05\)70267-x](https://doi.org/10.1016/s1473-3099(05)70267-x) | PubMed

2. Misiakos EP, et al. (2014) Current Concepts in the Management of Necrotizing Fasciitis. *Front Surg* **1** <https://doi.org/10.3389/fsurg.2014.00036> | PubMed
3. Gryllos I, et al. (2008) Induction of group A *Streptococcus* virulence by a human antimicrobial peptide. *Proc Natl Acad Sci* **105**:16755-16760 <https://doi.org/10.1073/pnas.0803815105> | PubMed
4. Tran-Winkler HJ, Love JF, Gryllos I, Wessels MR (2011) Signal Transduction through CsrRS Confers an Invasive Phenotype in Group A *Streptococcus*. *PLoS Pathog* **7**:e1002361 <https://doi.org/10.1371/journal.ppat.1002361> | PubMed
5. Love JF, Tran-Winkler HJ, Wessels MR (2012) Vitamin D and the Human Antimicrobial Peptide LL-37 Enhance Group A *Streptococcus* Resistance to Killing by Human Cells. *mBio* **3**:e00394-12 <https://doi.org/10.1128/mbio.00394-12> | PubMed
6. Brouwer S, et al. (2023) Pathogenesis, epidemiology and control of Group A *Streptococcus* infection. *Nat Rev Microbiol* **21**:431-447 <https://doi.org/10.1038/s41579-023-00865-7> | PubMed
7. Carroll RK, Musser JM (2011) From transcription to activation: how group A streptococcus, the flesh-eating pathogen, regulates SpeB cysteine protease production. *Mol Microbiol* **81**:588-601 <https://doi.org/10.1111/j.1365-2958.2011.07709.x> | PubMed
8. Ikebe T, et al. (2010) Highly Frequent Mutations in Negative Regulators of Multiple Virulence Genes in Group A Streptococcal Toxic Shock Syndrome Isolates. *PLoS Pathog* **6**:e1000832 <https://doi.org/10.1371/journal.ppat.1000832> | PubMed
9. Ikebe T, et al. (2016) Spontaneous mutations in *Streptococcus pyogenes* isolates from streptococcal toxic shock syndrome patients play roles in virulence. *Sci Rep* **6** <https://doi.org/10.1038/srep28761> | PubMed
10. Graham Morag R, et al. (2002) Virulence control in group A *Streptococcus* by a two-component gene regulatory system: Global expression profiling and *in vivo* infection modeling. *Proc Natl Acad Sci* **99**:13855-13860 <https://doi.org/10.1073/pnas.202353699> | PubMed
11. Gryllos I, et al. (2007) Mg²⁺ signalling defines the group A streptococcal CsrRS (CovRS) regulon. *Mol Microbiol* **65**:671-683 <https://doi.org/10.1111/j.1365-2958.2007.05818.x> | PubMed
12. Finn MB, Ramsey KM, Dove SL, Wessels MR (2021) Identification of Group A *Streptococcus* Genes Directly Regulated by CsrRS and Novel Intermediate Regulators. *mBio* **12**:e01642-21 <https://doi.org/10.1128/mbio.01642-21> | PubMed
13. Kahlenberg JM, Kaplan MJ (2013) Little Peptide, Big Effects: The Role of LL-37 in Inflammation and Autoimmune Disease. *J Immunol* **191**:4895-4901 <https://doi.org/10.4049/jimmunol.1302005> | PubMed
14. Dorschner RA, et al. (2001) Cutaneous Injury Induces the Release of Cathelicidin Anti-Microbial Peptides Active Against Group A *Streptococcus*. *J Invest Dermatol* **117**:91-97 <https://doi.org/10.1046/j.1523-1747.2001.01340.x> | PubMed
15. Schaubert J, et al. (2007) Injury enhances TLR2 function and antimicrobial peptide expression through a vitamin D-dependent mechanism. *J Clin Invest* **117**:803-811 <https://doi.org/10.1172/jci30142> | PubMed
16. Neely MN, Lyon WR, Runft DL, Caparon M (2003) Role of RopB in Growth Phase Expression of the SpeB Cysteine Protease of *Streptococcus pyogenes*. *J Bacteriol* **185**:5166-5174 <https://doi.org/10.1128/jb.185.17.5166-5174.2003> | PubMed
17. Do H, et al. (2017) Leaderless secreted peptide signaling molecule alters global gene expression and increases virulence of a human bacterial pathogen. *Proc Natl Acad Sci* **114** <https://doi.org/10.1073/pnas.1705972114> | PubMed
18. Ma Y, Bryant AE, Salmi DB, McIndoo E, Stevens D (2009) L. *vfr*, a Novel Locus Affecting Cysteine Protease Production in *Streptococcus pyogenes*. *J Bacteriol* **191**:3189-3194 <https://doi.org/10.1128/jb.01771-08> | PubMed

19. Shelburne Iii SA, et al. (2011) An amino-terminal signal peptide of Vfr protein negatively influences RopB-dependent SpeB expression and attenuates virulence in *Streptococcus pyogenes*. *Mol Microbiol* **82**:1481-1495 <https://doi.org/10.1111/j.1365-2958.2011.07902.x> | [PubMed](#)
20. LaRock CN, Nizet V (2015) Cationic antimicrobial peptide resistance mechanisms of streptococcal pathogens. *Biochim Biophys Acta BBA - Biomembr* **1848**:3047-3054 <https://doi.org/10.1016/j.bbamem.2015.02.010> | [PubMed](#)
21. Alberti S, Ashbaugh CD, Wessels MR (1998) Structure of the *has* operon promoter and regulation of hyaluronic acid capsule expression in group A *Streptococcus*. *Mol Microbiol* **28**:343-353 <https://doi.org/10.1046/j.1365-2958.1998.00800.x> | [PubMed](#)
22. Blöchl C, et al. (2021) Proteolytic Profiling of Streptococcal Pyrogenic Exotoxin B (SpeB) by Complementary HPLC-MS Approaches. *Int J Mol Sci* **23** <https://doi.org/10.3390/ijms23010412> | [PubMed](#)
23. Minns D, et al. (2021) The neutrophil antimicrobial peptide cathelicidin promotes Th17 differentiation. *Nat Commun* **12**:1285 <https://doi.org/10.1038/s41467-021-21533-5> | [PubMed](#)
24. Herwald H, et al. (2004) M Protein, a Classical Bacterial Virulence Determinant, Forms Complexes with Fibrinogen that Induce Vascular Leakage. *Cell* **116**:367-379 [https://doi.org/10.1016/s0092-8674\(04\)00057-1](https://doi.org/10.1016/s0092-8674(04)00057-1) | [PubMed](#)
25. Tanaka M, et al. (2020) Group A *Streptococcus* establishes pharynx infection by degrading the deoxyribonucleic acid of neutrophil extracellular traps. *Sci Rep* **10**:3251 <https://doi.org/10.1038/s41598-020-60306-w> | [PubMed](#)
26. Buchanan JT, et al. (2006) DNase Expression Allows the Pathogen Group A *Streptococcus* to Escape Killing in Neutrophil Extracellular Traps. *Curr Biol* **16**:396-400 <https://doi.org/10.1016/j.cub.2005.12.039> | [PubMed](#)
27. Nilsson M, et al. (2006) Activation of human polymorphonuclear neutrophils by streptolysin O from *Streptococcus pyogenes* leads to the release of proinflammatory mediators. *Thromb Haemost* **95**:982-990 <https://doi.org/10.1160/th05-08-0572> | [PubMed](#)
28. O'Donoghue AJ, et al. (2013) Global Substrate Profiling of Proteases in Human Neutrophil Extracellular Traps Reveals Consensus Motif Predominantly Contributed by Elastase. *PLoS ONE* **8**:e75141 <https://doi.org/10.1371/journal.pone.0075141> | [PubMed](#)
29. LaRock Doris L, Russell R, Johnson AF, Wilde S, LaRock CN (2020) Group A *Streptococcus* Infection of the Nasopharynx Requires Proinflammatory Signaling through the Interleukin-1 Receptor. *Infect Immun* **88**:e00356-20 <https://doi.org/10.1128/iai.00356-20> | [PubMed](#)
30. Hemmers S, Teijaro JR, Arandjelovic S, Mowen KA (2011) PAD4-Mediated Neutrophil Extracellular Trap Formation Is Not Required for Immunity against Influenza Infection. *PLoS ONE* **6**:e22043 <https://doi.org/10.1371/journal.pone.0022043> | [PubMed](#)
31. Guerra S, LaRock C (2024) Group A *Streptococcus* interactions with the host across time and space. *Curr Opin Microbiol* **77** <https://doi.org/10.1016/j.mib.2023.102420> | [PubMed](#)
32. Kasper KJ, et al. (2014) Bacterial Superantigens Promote Acute Nasopharyngeal Infection by *Streptococcus pyogenes* in a Human MHC Class II-Dependent Manner. *PLoS Pathog* **10**:e1004155 <https://doi.org/10.1371/journal.ppat.1004155> | [PubMed](#)
33. Do H, et al. (2024) Engineered probiotic overcomes pathogen defences using signal interference and antibiotic production to treat infection in mice. *Nat Microbiol* **9**:502-513 <https://doi.org/10.1038/s41564-023-01583-9> | [PubMed](#)
34. Belaouaj A (2002) Neutrophil elastase-mediated killing of bacteria: lessons from targeted mutagenesis. *Microbes Infect* **4**:1259-1264 [https://doi.org/10.1016/s1286-4579\(02\)01654-4](https://doi.org/10.1016/s1286-4579(02)01654-4) | [PubMed](#)
35. Aziz RK, et al. (2004) Invasive M1T1 group A *Streptococcus* undergoes a phase-shift *in vivo* to prevent proteolytic degradation of multiple virulence factors by SpeB. *Mol Microbiol* **51**:123-134 <https://doi.org/10.1046/j.1365-2958.2003.03797.x> | [PubMed](#)

36. Kansal RG, Nizet V, Jeng A, Chuang W.-J, Kotb M (2003) Selective modulation of superantigen-induced responses by streptococcal cysteine protease. *J Infect Dis* **187**:398-407 <https://doi.org/10.1086/368022> | PubMed
37. Lauth X, et al. (2009) M1 Protein Allows Group A Streptococcal Survival in Phagocyte Extracellular Traps through Cathelicidin Inhibition. *J Innate Immun* **1**:202-214 <https://doi.org/10.1159/000203645> | PubMed
38. LaRock DL, et al. (2022) Group A Streptococcus induces GSDMA-dependent pyroptosis in keratinocytes. *Nature* **605**:527-531 <https://doi.org/10.1038/s41586-022-04717-x> | PubMed
39. Bjånes E, et al. (2024) An efficient *in vivo*-inducible CRISPR interference system for group A *Streptococcus* genetic analysis and pathogenesis studies. *mBio* **15**:e00840-24 <https://doi.org/10.1128/mbio.00840-24> | PubMed
40. Klock HE, Lesley SA (2009) The Polymerase Incomplete Primer Extension (PIPE) Method Applied to High-Throughput Cloning and Site-Directed Mutagenesis. In: Doyle S. A. (Ed). *High Throughput Protein Expression and Purification* **498** Totowa, NJ: Humana Press. pp. 91-103 https://doi.org/10.1007/978-1-59745-196-3_6 | PubMed
41. Jeng A, et al. (2003) Molecular Genetic Analysis of a Group A *Streptococcus* Operon Encoding Serum Opacity Factor and a Novel Fibronectin-Binding Protein, SfbX. *J Bacteriol* **185**:1208-1217 <https://doi.org/10.1128/jb.185.4.1208-1217.2003> | PubMed
42. Wilde S, et al. (2023) Detoxification of reactive oxygen species by the hyaluronic acid capsule of group A *Streptococcus*. *Infect Immun* **91**:e00258-23 <https://doi.org/10.1128/iai.00258-23> | PubMed
43. LaRock CN, et al. (2016) IL-1 β is an innate immune sensor of microbial proteolysis. *Sci Immunol* **1** <https://doi.org/10.1126/sciimmunol.aah3539> | PubMed
44. Johnson AF, et al. (2025) Proinflammatory synergy between protease and superantigen streptococcal pyogenic exotoxins. *Infect Immun* **93**:e00405-24 <https://doi.org/10.1128/iai.00405-24> | PubMed
45. Sun J, et al. (2020) The *Pseudomonas aeruginosa* protease LasB directly activates IL-1 β . *EBioMedicine* **60** <https://doi.org/10.1016/j.ebiom.2020.102984> | PubMed

Peer reviews

Reviewer #1 (Public review):

Summary:

This manuscript examines how *Streptococcus pyogenes* regulates expression of the virulence factor SpeB in response to both bacterial and host-derived cues. The authors propose that Vfr acts as a repressor of speB expression and that degradation of Vfr by SpeB or by neutrophil-derived proteases relieves this repression. This creates a model in which *S. pyogenes* can sense proteolytic activity during infection and use that information to tune virulence factor expression.

Strengths:

The main strength of the study is the bacterial regulatory mechanism. The dual reporter system provides a useful way to follow speB and hasABC expression, and the genetic analysis of known regulators helps validate the system. The media-swap experiments, recombinant Vfr experiments, and SpeB-mediated degradation of Vfr support the conclusion that Vfr represses speB and that proteolysis can relieve this repression. The finding that SpeB can degrade Vfr is particularly interesting because it suggests an autoregulatory mechanism that could reinforce SpeB expression once it has been initiated.

Weaknesses:

The host side of the model is less completely supported. The authors show that neutrophil lysates and protease-containing fractions can induce the *speB* reporter and degrade Vfr, which supports the idea that neutrophil-derived proteases can affect this circuit. However, the *in vivo* interpretation relies heavily on PAD4-deficient mice to implicate neutrophil extracellular traps. PAD4 deficiency is a useful perturbation, but it does not by itself distinguish loss of extracellular trap formation from changes in neutrophil recruitment, survival, degranulation, phagocytosis, oxidative killing, or other neutrophil death pathways. As a result, the current data support a role for neutrophil-associated proteolytic activity more strongly than they support a specific role for extracellular traps. This distinction is important for interpreting the central model. The bacterial circuit is well developed, but the host-derived cue remains somewhat underdefined. If the relevant signal is extracellular protease activity more broadly, then the model is still interesting, but the conclusion should be framed around neutrophil-derived proteolytic stress rather than extracellular traps specifically. If extracellular traps are the key *in vivo* source of protease exposure, then additional evidence would be needed to separate that mechanism from other neutrophil effector functions that remain intact in PAD4-deficient cells.

Overall:

This is a valuable study with solid evidence for a bacterial protease-sensing regulatory mechanism controlling *SpeB* expression. The work should be useful to investigators interested in bacterial virulence regulation, host-pathogen interactions, and how pathogens integrate immune-derived cues during infection. The impact of the study would be stronger if the host-derived signal were defined more precisely, but the bacterial Vfr-*SpeB* circuit provides a compelling framework for thinking about how *S. pyogenes* links proteolytic activity to virulence gene expression.

<https://doi.org/10.7554/eLife.112023.1.sa2>

Reviewer #2 (Public review):

Summary:

The study examines how *Streptococcus pyogenes* integrates bacterial and host-derived signals to regulate *SpeB*, proposing that Vfr acts as a protease-sensitive repressor whose degradation relieves repression of *speB*. The authors further suggest that neutrophil-derived serine proteases, including those associated with inflammatory conditions, may promote this transition, and thereby counterbalance LL-37/CovRS-associated suppression of *speB*. The conceptual framework is interesting and potentially important for understanding how host inflammation feeds into bacterial virulence regulation.

Strengths:

The work addresses a biologically significant question and does so using a broad and generally well-integrated experimental approach, including bacterial genetics, reporter assays, recombinant protein analyses, neutrophil-derived material, human blood infection, and mouse infection models. A particular strength is the effort to connect host inflammatory processes to bacterial regulatory behavior, which gives the study conceptual reach beyond a narrow mechanistic observation. The data support the view that Vfr is relevant to *speB* control and that neutrophil-associated protease activity may influence this pathway.

Weaknesses:

The main limitations are mechanistic. The physiological form, localization, and abundance of Vfr are not sufficiently defined to support the proposed model at full strength, and the evidence that Vfr functions as a *SpeB*-labile repressor under biologically relevant conditions

remains incomplete. The relationship between Vfr and the broader RopB/SIP regulatory framework is also not yet firmly established. In addition, the reporter system is not yet benchmarked closely enough against endogenous SpeB protein output, and its growth-phase dependence is insufficiently resolved, which makes it difficult in some settings to distinguish promoter activity from mature protease production. The neutrophil protease component is likewise not defined beyond a general serine protease signal, and the potentially important LL-37/CovRS/Vfr connection is underdeveloped in the main text. Overall, the conceptual advance is promising, but several of the central mechanistic claims would benefit from more direct experimental support and more cautious framing.

<https://doi.org/10.7554/eLife.112023.1.sa1>

Reviewer #3 (Public review):

Summary:

SpeB is a cysteine protease secreted during infection by *Streptococcus pyogenes* (Spy). SpeB has been extensively investigated for its role in pathogenesis, which involves proteolytic processing of both Spy virulence factors and host proteins. Regulation of speB expression is complex and includes growth phase regulation, a quorum-sensing system, the transcription factor RopB, and the global regulatory system CovRS (CsrRS). Guerra et al now attempt to refine the current model of regulation of SpeB expression, focusing on the Spy protein Vfr, which has been suggested previously to act as a negative regulator of SpeB expression. In the current study, neutrophil lysates (representing proteases released during NETosis) are shown to degrade Vfr and to relieve repression of SpeB. At high cell density, SpeB itself also degrades Vfr, which may allow autoregulation of SpeB expression. These observations are unsurprising as the broad protease activities of both neutrophil proteases and SpeB are well known. Nonetheless, the data presented fill in additional details in our understanding of the complex regulation of an important Spy virulence factor.

Strengths:

- (1) Construction of a GFP reporter strain provided a facile methodology for tracking speB promoter activity in a variety of experimental setups.
- (2) A Vfr deletion mutant was a useful tool to investigate the role of Vfr in SpeB regulation, and mutants in speB and ropB were important controls.
- (3) Experiments using neutrophil lysates in vitro, as well as in vivo studies of mice depleted of neutrophils with anti-Ly6G or in PAD4^{-/-} mice (that cannot form NETs) support the hypothesis that neutrophil proteases derepress speB expression by degrading Vfr.

Weaknesses:

- (1) The introduction and all the experiments in Figure 1 focus on CovRS, which turns out to be largely tangential to the overall story developed by the rest of the study. On the other hand, the complex and well-studied regulation of speB expression by RopB and the SIP quorum-sensing system is only minimally described. A better framing would be a more detailed introduction to the current model of speB/RopB/SIP/quorum sensing/growth phase regulation. CovRS could be introduced later as its relevance is really just to show that neutrophil lysates or NETs do more than simply providing LL-37, which signals through CsrS, as another regulator of speB expression.
- (2) Vfr, as the central focus of the paper, also deserves a more thorough introduction to provide context for the study. For example, reference 19 (Shelburne et al, 2011) showed reduced transcription of speB in a vfr mutant, an effect that could be complemented by expressing vfr or a 39-aa N-terminal fragment in trans. That study presented evidence that

the N-terminal peptide binds to RopB, which may prevent RopB from upregulating SpeB expression. Do the authors concur with that model? As it stands, the discussion and model in Figure 1A imply a direct regulatory effect of Vfr on speB expression rather than an indirect one through regulation of RopB. If direct regulation of speB by Vfr is a consideration, it should be investigated more thoroughly, e.g., by promoter-binding assays, CHIP-seq, etc.

(3) Use of single-cell flow cytometry generally confirmed results observed in batch culture. The authors also comment repeatedly on the heterogeneity of individual cell fluorescence representing both speB and has operon expression. However, the reason(s) for heterogeneity in gene expression are not explored, e.g., differences in individual cell growth rate in batch culture, variable loss of reporter plasmid during infection experiments, etc).

(4) Lines 116-118 and Figure 3C: Incubation of recombinant Vfr with Spy Dvfr reduced SpeB expression, but the degree of suppression is modest compared to that seen in wild-type Spy. How does the concentration of rVfr added compare to that present in the culture fluid of wild-type Spy? (Also, the concentration of rVfr used is unclear: the figure says 3 µg/ml and the legend says 0.3 mg/ml, i.e., 300 µg/ml).

(5) Lines 125-126: "...the Vfr structure contains several potential protease SpeB cleavage sites..." The role of Vfr in degrading SpeB could be clarified by identifying the predicted cleavage products, e.g., by mass spec, after co-incubation of the two recombinant proteins.

(6) Lines 122-124: "Notably, speB expression in Spy Dvfr is unaffected by LL-37 or MgCl₂, further validating its [Vfr's?] dominance over CovRS regulation." This statement is an oversimplification and is potentially misleading: LL-37 is degraded by SpeB (Nyberg et al, JBC 2004), which likely explains why the addition of LL-37 fails to signal through CovRS to repress SpeB in Spy Dvfr since SpeB is produced continuously in that strain. By contrast, SpeB is only produced during the stationary phase in the wild type, so LL-37 remains active throughout the exponential phase and represses SpeB expression. The response to the CovRS ligand MgCl₂ is similar (or greater) in Spy Dvfr compared to wild type (Figure S2C).

(7) Lines 153-154 and Figure 6E: Growing wild type Spy in the presence of neutrophil lysates with or without a protease inhibitor stimulated or repressed speB expression in a manner consistent with degradation (or not) of Vfr. It would be confirmatory and informative to do the same experiment with the Spy Dvfr strain.

(8) Clarity of writing could be improved, particularly by eliminating pronouns of indefinite reference (it, its, this) in contexts in which the subject is ambiguous (examples at lines 62, 89, 111, 114, 115, 123, 183, 190, 193, 204, 205, 210, 217, 221, 222, 224).

<https://doi.org/10.7554/eLife.112023.1.sa0>